

Surface-induced nonlinearities of liquid crystals driven by an electric fieldL. Lucchetti,^{*} M. Gentili, and F. Simoni*Dipartimento di Fisica e Ingegneria dei Materiali e del Territorio and CNISM, Università Politecnica delle Marche, Via Brecce Bianche, 60131 Ancona, Italy*

S. Pavliuchenko, S. Subota, and V. Reshetnyak

Physics Faculty, Kyiv National Taras Shevchenko University, Prosp. Glushkova 2, building 1, Kyiv, 03022, Ukraine

(Received 28 April 2008; published 23 December 2008)

We report the study of the effect of a static electric field on the huge optical nonlinearity of methyl-red doped nematic liquid crystals. Experimental data are well fitted using a theoretical model that takes into account the modulation of the surface charge density due to the impinging light beam. It is demonstrated that the optical nonlinearity can be varied by orders of magnitude with application of a low voltage below the threshold of the Fredericks transition. These results confirm the previously proposed model of surface induced nonlinear effects.

DOI: [10.1103/PhysRevE.78.061706](https://doi.org/10.1103/PhysRevE.78.061706)

PACS number(s): 42.70.Df, 42.65.-k

I. INTRODUCTION

The nematic liquid crystal pentyl-cyanobiphenil (5CB) doped with the azo dye methyl red (MR) is able to exhibit an optical nonlinearity among the highest ever observed in organic media [1]. The first observation was made by Khoo and co-workers in cells with homeotropic configuration. They defined the observed behavior as “supranonlinear” and gave a first explanation based on a photorefractivelike effect sustained by an internal dc field [2]. In the paper of Khoo a nonlinear refractive index $n_2 > 1 \text{ cm}^2/\text{W}$ was measured, five orders of magnitude higher than the one typical of pure nematics leading to the well known giant optical nonlinearity [3]. Several further experiments have confirmed the supranonlinear response and have highlighted the crucial role played by the cell surface in determining such a high nonlinearity. The effect has been phenomenologically described as a surface-induced nonlinear effect and called SINE [4]. The phenomenon leading to the transient interfacial modification responsible for SINE is connected to the light-induced adsorption and desorption of MR molecules at the irradiated surface [5,6]. In particular, it has been recently demonstrated that during cell filling with the LC-dye mixture, a layer of dye molecules about 6 nm thick adsorbs on the cell surfaces [7]. This layer is actually a photosensitive layer that exhibits an anisotropy along the filling direction. The subsequent cell irradiation with polarised light of wavelength in the dye absorption band gives rise to further adsorption and/or desorption of dye molecules with a prevalence of one of the two processes depending on light intensity and polarization. Adsorption and desorption of MR molecules give rise to the modification of the surface conditions responsible for the nonlinear response of the liquid crystal.

In specific conditions (thin cells with very weak anchoring) the SINE effect gives rise to nonlinear coefficients n_2 up to $10^3 \text{ cm}^2/\text{W}$, a behavior referred to as colossal optical nonlinearity [1,8]. The possibility of using colossal optical non-

linearity for applicative purposes has been successfully demonstrated in optical phase conjugation experiments devoted to wave front correction of weak light beams [9]. More recently we have shown the possibility of controlling the optical nonlinear response of 5CB+MR cells in wave mixing experiments by means of an external low frequency electric field. The field applied perpendicular to the cell substrates allows reproducibility of the colossal nonlinear response without any critical control of the cell interfaces [10].

On the other hand, the effect of electric field on colossal nonlinearity has been investigated only in the conventional wave mixing geometry leading to a transient nonlinear grating. For this reason a study of the nonlinear behavior of a MR-doped nematic cell in a single beam experiment under application of a dc voltage is important to clarify the origin of the nonlinearity and the potential exploitation of the effect for optical processing devices. In fact the ability of controlling colossal optical nonlinearity in single beam configuration would be extremely interesting for realization of light valves of simplified geometry and enhanced performances. A possible drawback may come from the need of using thin cells which, even with high value of n_2 , produce a small nonlinear phase shift.

Based on this motivation we have studied the self-phase modulation (SPM) of a Gaussian beam incident on a planar aligned cell filled of 5CB doped by MR in the presence of an external dc field. According to a previously presented model [10] a Gaussian laser beam is expected to create a modification of the irradiated surface and the dc field is expected to produce a molecular reorientation dependent on the pattern created by light on the same surface. Both the experimental results and a theoretical model confirm this prediction.

The paper is organised as follows. Section II concerns the experiments: details on the samples and experimental data are reported. In Sec. III we present the theoretical model and compare its predictions to the measured parameters, showing an excellent agreement between theory and experiments. Conclusions are drawn in Sec. IV.

^{*}l.lucchetti@univpm.it

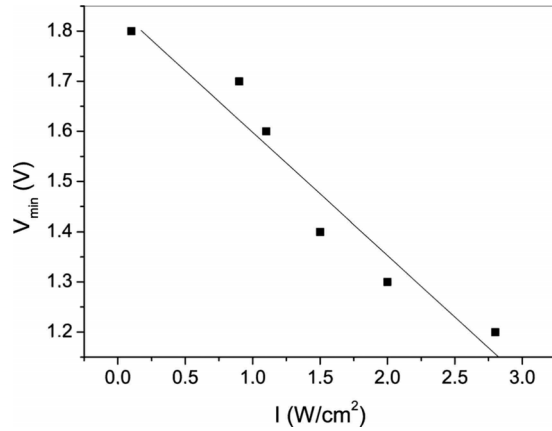


FIG. 1. (Color online) Minimum value of the applied voltage required to observe self-phase modulation vs incident intensity. The line is a linear fit of the experimental points. Cell thickness is $d = 14 \mu\text{m}$.

II. EXPERIMENTAL INVESTIGATION

Experiments have been carried out on 5CB planar cells doped with a small amount of MR. The dye weight concentration is 0.1% since a higher dye content would lead to memory effects, not desirable in the present case. The planar alignment has been obtained by treating one glass substrate with polyvinyl alcohol and then rubbing it and leaving the other substrate uncoated. In this way one gets cells with a good planar alignment and a surface with very low anchoring energy, allowing the use of low incident intensity to observe the nonlinear behavior [1]. Both glass substrates have a ITO coating. Cell thickness has been controlled by Mylar spacers and carefully measured by means of spectroscopic techniques. It has been varied from 10 to $100 \mu\text{m}$, in order to test the dependence of the observed effect on the sample thickness.

The experimental setup is the one commonly used to observe SPM [11]. A pump beam from a cw Nd:YVO₄ frequency doubled laser ($\lambda = 532 \text{ nm}$) is focused by a 22 cm planoconvex lens on the sample untreated surface at normal incidence. The beam is polarized in order to impinge the sample as a pure extraordinary wave. The incident power was varied between 30 and $1300 \mu\text{W}$, corresponding to intensities in the range (0.8–40) W/cm^2 . It is worth noting that the intensity typically needed to observe SPM in pure liquid crystals is of the order of 10^2 – $10^3 \text{ W}/\text{cm}^2$ [11,12]. A dc voltage below the electric Fredericks threshold is applied perpendicular to the cell substrates.

The typical SPM pattern is easily observed in all the analyzed cells even at the lowest intensity, but only if the external bias V is switched on. The rise time of the signal is typically on the order of a few seconds. The minimum value of V required to observe the effect depends on the impinging intensity as shown in Fig. 1 and is in the range (1.2–1.8) V. These values are below the threshold for the electric Fredericks transition, which has been directly measured to be about 4 V when no light beam is impinging on the sample. This means that not only the incident light does not produce any distortion in the absence of the external bias, but also the

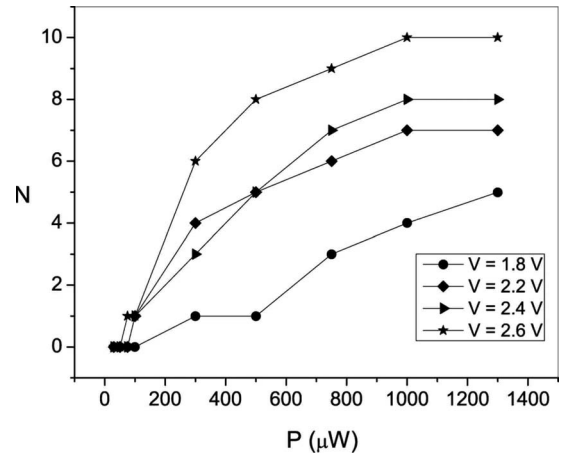


FIG. 2. Number of SPM rings N vs incident power for four different values of the external voltage. Cell thickness is $d = 35 \mu\text{m}$.

external bias does not produce any distortion in the absence of laser light. (Note that the presence of the dopant produces an increase of about one order of magnitude of V_{th} due to charge screening effects.)

Once the ring pattern has been obtained, the number of rings N can be controlled by means of the external bias. In particular, an increase of V leads to an increase of N . As an example, Fig. 2 shows N versus the incident power for several values of V , for a $35 \mu\text{m}$ cell. It is evident that larger number of rings corresponds to higher V and, of course, to higher laser power. The dependence of N on V is also evident in Fig. 3 where several images recorded at different times correspondent to different values of the applied voltage are reported. The images are subsequent photograms extracted from a ccd movie recorded at fixed intensity ($I = 5 \text{ W}/\text{cm}^2$) while V increased from 0 to 2.6 V. Note that the bias can be increased up to about 2.8 V, then the SPM pattern collapses.

The number of SPM rings is linked to the maximum induced birefringence Δn . In fact the maximum phase shift induced by the incident light can be expressed as $\Delta\varphi = 2\pi N$ [11]. Since $\Delta\varphi = \frac{2\pi}{\lambda} d\Delta n$, one gets $\Delta n = \frac{N\lambda}{d}$. Using this latter relation, it is possible to plot Δn vs I for each cell and for each value of the external bias. An evaluation of the experimental errors associated with Δn has shown that they are not higher than 10^{-3} , that is at least one order of magnitude lower than the obtained values of the induced birefringence. Figure 4 reports these curves for two cells: one of thickness $d = 10 \mu\text{m}$ [Fig. 4(a)] and one of thickness $d = 60 \mu\text{m}$ [Fig. 4(b)]. As it can be seen, the induced birefringence Δn increases with I and also with V for fixed values of I , as expected.

By comparing the different curves it is easy to notice that the thinner is the cell the higher is the sensitivity. Moreover, the maximum values of the induced birefringence are much higher in the thinner cell reaching in one case the value $\Delta n = 0.19$ that is equal to the total intrinsic birefringence of 5CB within the experimental errors. (Note that for $\Delta n = 0.19$, the relation $d_{\text{min}} = \frac{\lambda}{\Delta n}$ gives $d_{\text{min}} \cong 3 \mu\text{m}$. This means that in highly nonlinear media, as dye doped liquid crystals are, SPM can be observed with cell thicknesses much lower than those typically used in undoped samples.)

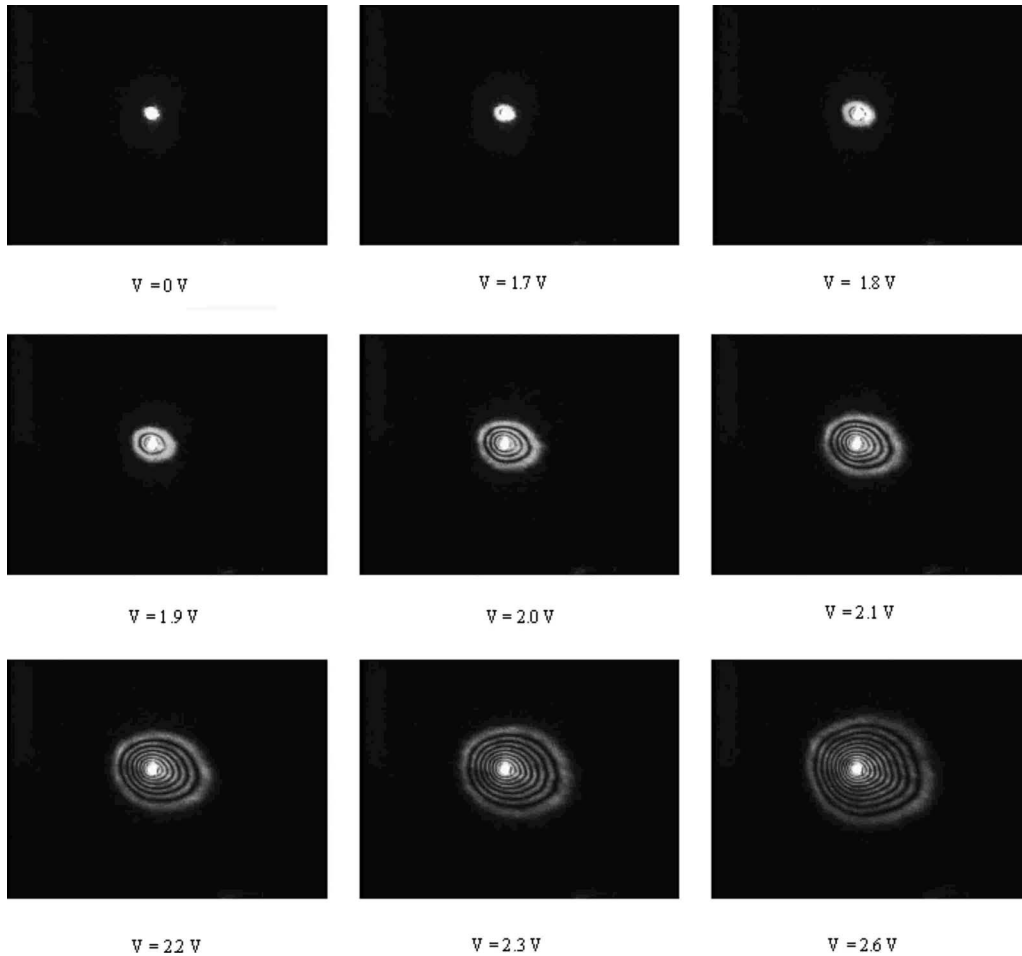


FIG. 3. Subsequent photographs showing the evolution of SPM pattern with the applied voltage. The incident intensity has a fixed value $I=5 \text{ W/cm}^2$. Cell thickness is $d=35 \mu\text{m}$.

Starting from the curves reported in Fig. 4 it is possible to evaluate the nonlinear coefficient n_2 . In fact, far from saturation a linear fit through the equation $\Delta n = n_2 I$ (valid for Kerr media [13]) can be performed. A typical example is reported in Fig. 5 for a $10 \mu\text{m}$ cell at $V=2.5 \text{ V}$. In this case the fitting parameter n_2 is $0.12 \text{ cm}^2/\text{W}$.

The dependence of Δn on the applied voltage V leads to a dependence of the nonlinear coefficient on the same parameter, as shown in Fig. 6. Here the error bars are the errors indicated by the fitting procedure carried out to determine n_2 from $\Delta n(I)$. Figure 6 clearly shows that by acting on V it is possible to change n_2 up to two orders of magnitude. The nonlinear coefficient ranges from 1.7×10^{-2} to $1 \times 10^{-1} \text{ cm}^2/\text{W}$ in the $10\text{-}\mu\text{m}$ -thick cell, and from 6×10^{-4} to $3 \times 10^{-2} \text{ cm}^2/\text{W}$ in the $60\text{-}\mu\text{m}$ -thick one. One can calculate the focal length of a nonlinear liquid crystal cell through the relation [13]:

$$f^{-1} = \frac{n_2}{n^o} \frac{d}{\xi^2} I, \quad (1)$$

where d is the cell thickness, ξ is the spot size on the sample, I is the incident intensity and n^o is the linear part of the refractive index. In case of the $60\text{-}\mu\text{m}$ -thick cell a focal

length f varying from 2.4 to 0.05 cm at a fixed intensity $I = 3 \text{ W/cm}^2$ is obtained with a bias variation of only 1 V.

III. DISCUSSION AND THEORETICAL MODEL

Experimental results clearly show that the ring pattern typical of SPM can be easily obtained in the studied samples, provided that a static field below the electric Fredericks threshold is applied. The required pump intensity and the minimum cell thickness are much lower than those usually needed for SPM experiments in pure nematics. Moreover, the thinner cells are more sensitive than the thicker ones and are characterised by higher values of the induced birefringence, in agreement with all the experimental observations made so far on 5CB doped with MR, which have led to the formulation of the SINE model [4]. In this model the origin of the supranonlinear or even colossal nonlinearities of these samples is considered to be the light-induced modulation of the surface conditions that in turn affects the director orientation in the bulk. Namely there is no direct optical torque on the LC molecules, but reorientation occurs due to the elasticity of the medium.

We have recently demonstrated that the optical nonlinear response of MR doped 5CB cells is easily controllable in

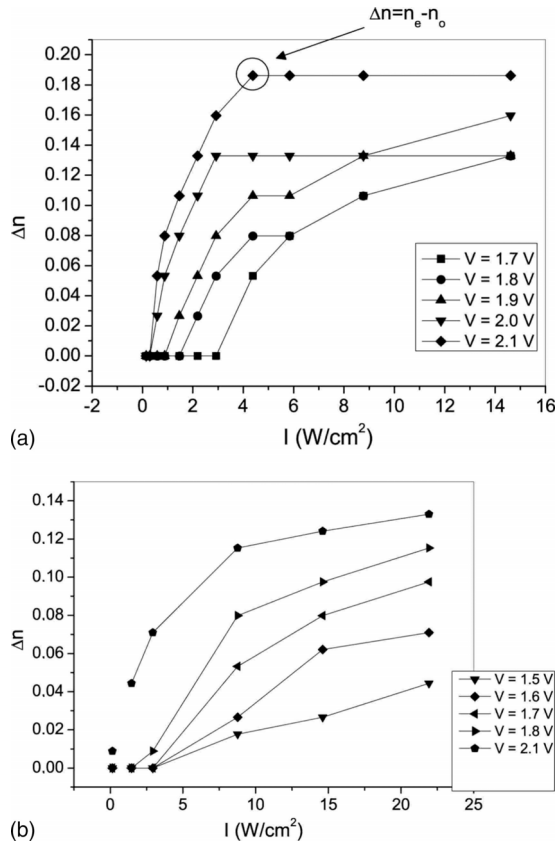


FIG. 4. (Color online) Light-induced birefringence Δn vs incident intensity for five values of the applied voltage. Cell thickness is $d = 10 \mu\text{m}$ in Fig. 4(a) and $d = 60 \mu\text{m}$ in Fig. 4(b).

wave mixing configuration, by an external electric field [10]. The model proposed takes into account the dependence of the effective internal voltage V_{bulk} on the surface charge density of ions, described by the relation

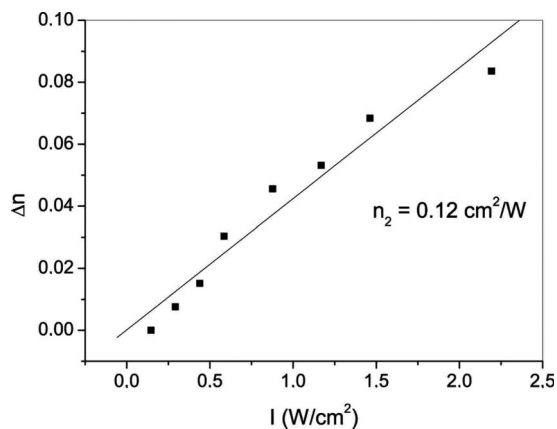


FIG. 5. Example of the linear fit for the evaluation of the nonlinear optical coefficient n_2 . The external voltage is $V = 2.5 \text{ V}$ and cell thickness is $d = 10 \mu\text{m}$.

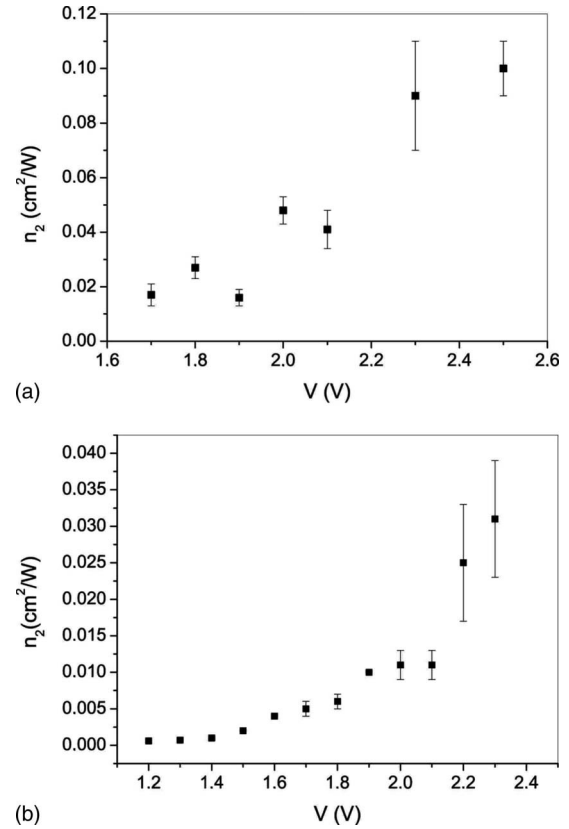


FIG. 6. Nonlinear optical coefficient n_2 vs applied voltage. Cell thickness is $d = 10 \mu\text{m}$ in Fig. 4(a) and $d = 60 \mu\text{m}$ in Fig. 4(b).

$$V_{\text{bulk}} \propto \left(V - 2 \frac{\sigma q d}{\epsilon_s} \right), \quad (2)$$

where V is the externally applied voltage, ϵ_s the surface dielectric constant, and σq the surface charge density of ions collected in front of each electrode [14].

In our experimental configuration, light-induced desorption of dye molecules from the irradiated surface is expected to be dominant on adsorption [15]. This effect reduces the surface density of dark adsorbed dye molecules [7,16]. Since there are several experimental demonstrations that dye-doping form charge complexes in liquid crystals [10,17–21], this layer is expected to have a polar character. Therefore the light-induced desorption reduces the surface charge density. As a consequence one gets a lowering of the screening effect, thus increasing the effective internal voltage. In this way the reduction of charge screening gives rise to a reduction of the actual Fredericks threshold. In other words, due to the Gaussian profile of the beam the threshold field results lower in correspondence of the Gaussian peak where the intensity is higher, and higher in correspondence of the tails. As a consequence the applied dc field produces a director distortion toward the homeotropic configuration only in the centre of the pump beam. A schematic representation of the situation is reported in Fig. 7. Figure 7(a) shows the cell and the index profile before voltage application. Director orientation is planar all over the sample and the refractive index is everywhere equal to n_e . When an external bias lower than the

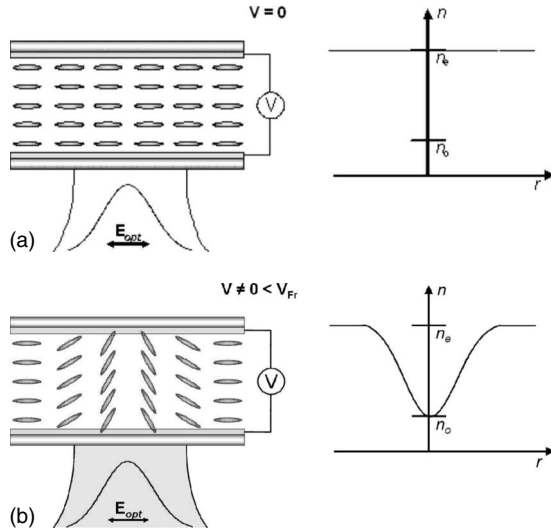


FIG. 7. Schematic representation of cell configuration and index profile under the action of only the optical field [Fig. 7(a)] and of both the optical field and the external voltage [Fig. 7(b)].

Fredericks transition voltage is applied [Fig. 7(b)] the induced distortion gives rise to the index profile reported, which in turn produces SPM of the incoming beam. In this way the Fredericks threshold voltage $V_{th}(I)$ depends on the impinging light intensity, being maximum at $I=0$. Therefore by increasing the bias voltage the director distortion increases thus increasing Δn and the number of rings until V approaches $V_{th}(0)$. At this stage the whole sample can be reoriented and the index modulation through the beam cross section decreases and becomes negligible at higher voltages, corresponding to the collapse of the SPM pattern observed in the experiment (saturation of the director orientation). A similar behavior can be observed if the voltage is kept at a value $V < V_{th}(0)$. No reorientation occurs if no light beam is impinging on the sample ($I=0$). By increasing the light intensity the SPM pattern appears following the typical growth (in rings number and diffraction angle) until saturation.

Let us proceed with analytical steps in order to obtain a quantitative comparison to the experimental data. Let us consider a planar aligned LC cell of thickness d with a dc voltage V applied. This voltage is partially screened due to the presence of charged impurities, so that the effective bulk voltage is $U_0 < V$. The cell is also illuminated by light with Gaussian distribution of intensity

$$I(r) = I(0)\exp(-r^2/w^2). \quad (3)$$

We assume that under illumination the electric field screening is partially reduced and the electric field potential at the illuminated substrate ($z=d$) takes the form

$$\Phi(z=d, r) = U_0 + U_1 \exp(-r^2/w^2). \quad (4)$$

The second term on the right side of Eq. (4) is the additional potential due to the light-induced lowering of the screening effect. From data of Fig. 1 we see that the minimum voltage required to observe the effect at a given value of intensity has a linear dependence on I with negative slope. Therefore we assume U_1 to be linear on the incident intensity, that is

$U_1 = u_0 + \alpha I$ where α and u_0 are constants to be evaluated starting from the experimental data. In other words, we expect that the applied voltage is initially totally screened by each electric double layer at the top and bottom substrates, so we do not observe any reorientation without light. When the optical field is switched on, the incident light somehow neutralizes the double layer at the irradiated surface. We assume that this “neutralization” is proportional to light intensity. It is worth noting that the linear assumption is not valid near the zero intensity region. This is evident in Fig. 1, where a linear extrapolation to zero intensity would give a threshold voltage of about 2 V, instead of the measured 4 V. The physical reason lies on the light-induced desorption of MR molecules which depends on the light irradiation dose [22] and is likely to have a thresholdlike behavior. So the linear assumption can be considered valid after the onset of the effect.

Before director distortion takes place, LC director at the top and bottom substrates is parallel to the OX axis. We describe director by polar and azimuthal angle $\mathbf{n} = (\cos \theta \cos \phi, \cos \theta \sin \phi, \sin \theta)$ and assume strong anchoring at the bottom substrate with easy axis given by $\mathbf{d}_1 = (\cos \theta_1, 0, \sin \theta_1)$ and weak finite anchoring with some easy axis directions $\mathbf{d}_2 = (\cos \theta_2, 0, \sin \theta_2)$ at the top substrate irradiated by laser light.

Neglecting the contributions of the optical field and flexopolarization to the total free energy, one gets

$$F = F_{\text{elastic}} + F_E + F_S, \quad (5)$$

where $F_E = -\frac{1}{2} \int (\mathbf{E} \cdot \hat{\epsilon} \mathbf{E}) dV$ and $F_S = -\frac{1}{2} W_2 \int (\mathbf{n} \cdot \mathbf{d}_2)^2 dS_2$ are, respectively, the contribution of the dc field and the surface term. The elastic free energy has the usual expression in one elastic constant approximation. We consider the case $\phi(r, \varphi, z) \equiv 0$, where φ is the azimuthal angle in a cylindrical frame. Polar angle θ and electric field potential Φ depend on the two coordinates z and r ; the electric field is determined by its potential in the usual way $\mathbf{E} = -\nabla \Phi$.

Using the expressions for div and curl in the cylindrical frame

$$\begin{aligned} \text{div } \mathbf{n} &= \frac{1}{r} \frac{\partial}{\partial r} (r \cos \theta) + \cos \theta \frac{\partial \theta}{\partial z}, \\ \text{curl } \mathbf{n} &= \left(-\sin \theta \frac{\partial \theta}{\partial z} - \cos \theta \frac{\partial \theta}{\partial r} \right) \mathbf{e}_\phi + \frac{1}{r} \frac{\partial}{\partial r} (r \cos \theta) \mathbf{e}_z \end{aligned} \quad (6)$$

one obtains the following Euler-Lagrange equation for the polar angle $\theta(r, z)$:

$$\begin{aligned} K \left[\frac{1}{r} \frac{\partial}{\partial r} \left(r \frac{\partial \theta}{\partial r} \right) + \frac{\partial^2 \theta}{\partial z^2} \right] - \epsilon_0 \epsilon_a \left(\cos \theta \frac{\partial \Phi}{\partial r} + \frac{\partial \Phi}{\partial z} \sin \theta \right) \\ \times \left(\sin \theta \frac{\partial \Phi}{\partial r} - \cos \theta \frac{\partial \Phi}{\partial z} \right) = 0, \end{aligned} \quad (7)$$

which should be accompanied by the Poisson equation for electric field potential $\Phi = \Phi(r, z)$

$$\nabla \cdot (\hat{\epsilon} \nabla \Phi) = 0. \quad (8)$$

In Eq. (8)

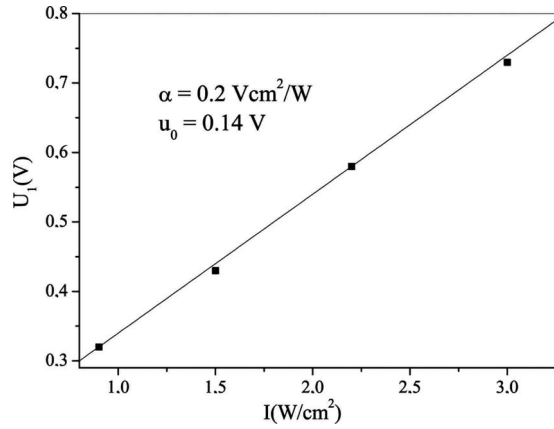


FIG. 8. Linear fit of the curve U_1 vs incident intensity. The value of V_0 is kept equal to 1.8 V.

$$\tilde{\epsilon} = \begin{pmatrix} \tilde{\epsilon}_\perp + \tilde{\epsilon}_a \cos^2 \theta & 0 & \tilde{\epsilon}_a \cos \theta \sin \theta \\ 0 & \tilde{\epsilon}_\perp & 0 \\ \tilde{\epsilon}_a \cos \theta \sin \theta & 0 & \tilde{\epsilon}_\perp + \tilde{\epsilon}_a \sin^2 \theta \end{pmatrix}. \quad (9)$$

If the beam width is bigger than cell thickness it is possible to neglect the derivative $\partial/\partial r$ compared to the derivative $\partial/\partial z$ and rewrite Eq. (7) in the following way:

$$K \left(\frac{\partial^2 \theta}{\partial z^2} \right) + \epsilon_0 \epsilon_a \left(\frac{\partial \Phi}{\partial z} \right)^2 \sin \theta \cos \theta = 0. \quad (10)$$

Equation (8) also simplifies to

$$\frac{\partial}{\partial z} \left(\tilde{\epsilon}_\perp + \tilde{\epsilon}_a \sin^2 \theta \frac{\partial \Phi}{\partial z} \right) = 0. \quad (11)$$

These two equations should be solved numerically with the following boundary conditions

$$\Phi(z=0, r) = 0, \quad \Phi(z=d, r) = U_0 + U_1 \exp(-r^2/d^2),$$

$$\theta(z=0, r) = \theta_1,$$

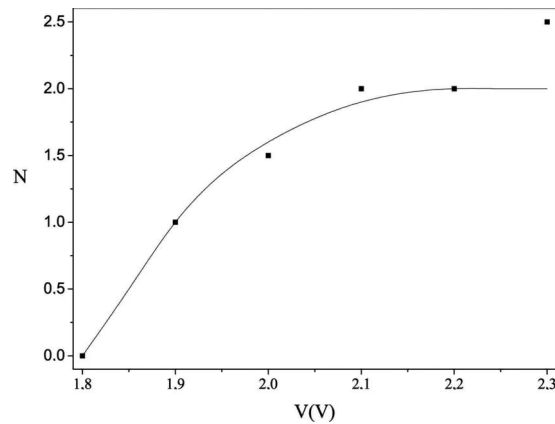


FIG. 9. Comparison between the expected number of SPM rings and those experimentally observed for $V_0=1.8$ V and $\alpha = 0.26$ Vcm²/W. The incident intensity is $I=1.5$ W/cm².

$$\left. \frac{\partial \theta}{\partial z} + \frac{W_2}{K} \sin \theta \cos \theta \right|_{z=d} = 0. \quad (12)$$

Note that due to the approximation made in Eq. (10), the model properly describes the behavior of the thinner cells for which $d < w$.

In order to find the director profile under light irradiation it is necessary to make some assumption about the values of U_0 and U_1 and about their dependence on light intensity. We

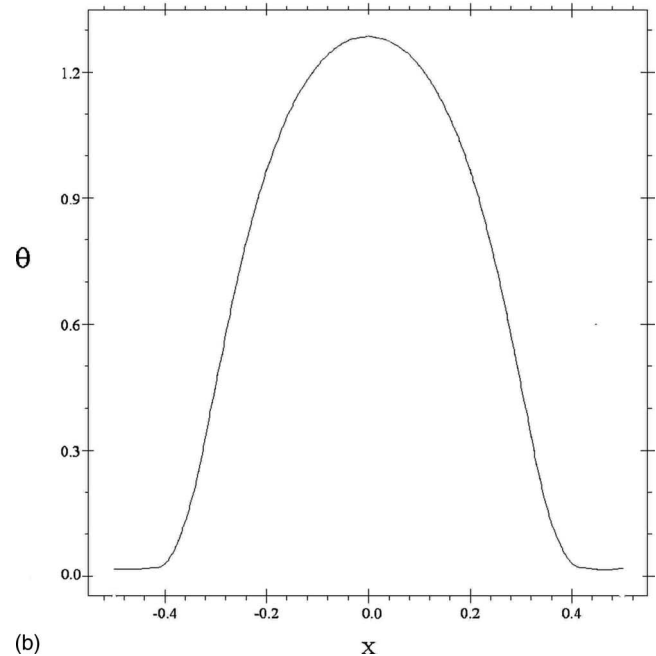
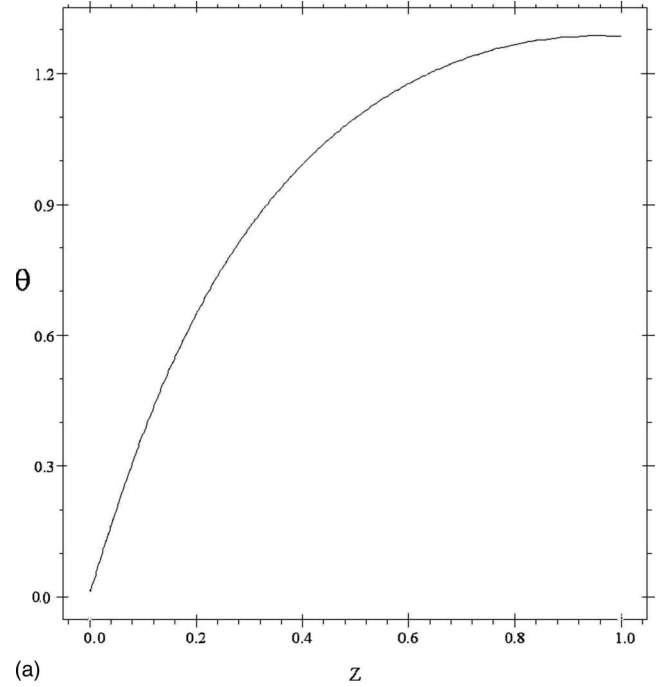


FIG. 10. Director profile along the cell thickness [Fig. 10(a)] and on the irradiated surface [Fig. 10(b)]. The abscissa is $Z=z/d$ in Fig. 10(a) and $X=x/(3w)$ in Fig. 10(b).

suppose that $U_0 = V - V_0$ and $U_1 = u_0 + \alpha I$, where the constants V_0 , α , and u_0 should be determined from the best fit of the experimental curves.

Using numerical solution for the system of Eqs. (10) and (11) for each given experimental value of the light intensity, we find the value of V_0 and a set of values $U_1(I)$ that give the best agreement between the expected number of SPM rings and the experimental data. We find $V_0 = 1.8$ V, which means that a large amount of the applied voltage is actually screened by charged impurities and dopant, as expected. The best values for the constants α and u_0 are $u_0 = 0.14$ V and $\alpha = 0.2$ V cm²/W, as shown in Fig. 8 where the linear fit of $U_1(I)$ is reported at $V_0 = 1.8$ V. The linear fit has been performed taking into account that the linear dependence cannot be extrapolated at zero intensity, as remarked above.

Figure 9 is an example of the comparison between the expected number of rings vs applied voltage for these values of V_0 , α , and u_0 , and those experimentally observed in case of $I = 1.5$ W/cm² and $d = 10$ μ m. The former have been calculated from the expected phase shift between the beam edge where there is no director reorientation ($n = n_e$) and the beam center where $n = n_{\text{eff}}(z, r)$:

$$\Delta\varphi = \frac{2\pi}{\lambda} \int_0^L [n_e - n_{\text{eff}}(z, r)] dz. \quad (13)$$

Numerical solution for $\theta(z, r)$ have been used for the evaluation of this phase shift.

In Fig. 9 $U_0 = (V - 1.8)$ V and $U_1 = 0.44$ V, that is the maximum voltage at the irradiated surface is $\Phi(z = d, r = 0) = (V - 1.4)$ V. The agreement between theory and experiment is very good.

The director profile in terms of the angle $\theta(r, z)$ along the cell thickness in correspondence of the center of the Gaussian beam and on the irradiated surface is reported in Fig. 10. The abscissa is $Z = z/d$ in Fig. 10(a) and $X = x/(3w)$ in Fig. 10(b). This means that $Z = 0$ corresponds to the surface with strong planar anchoring and $Z = 1$ to the surface with finite weak anchoring irradiated by light. Moreover, $X = \pm 0.4$, cor-

responds to $x = \pm 1.2w$, i.e., the induced distortion is slightly wider than the incident beam, as expected. The director profile along cell thickness [Fig. 10(a)] is calculated in correspondence of the centre of the Gaussian distribution where the induced distortion is expected to be maximum, whereas that on the irradiated surface [Fig. 10(b)] is calculated between the edges of the induced distortion. The parameters used in the calculation of $\theta(r, z)$ are $U_0 = 0.2$ V, $U_1 = 0.57$ V (corresponding to $I = 2.15$ W/cm²) and $d = 10$ μ m.

The dependence of θ on X is in perfect agreement with the expected index profile shown in Fig. 7.

IV. CONCLUSIONS

We have studied the nonlinear optical behavior of MR-doped 5CB cells when a static electric field is applied. We have presented a model where the photosensitive dark adsorbed layer of dye molecules acts as charge screening with respect to the applied voltage. The light-induced desorption reduces the screening effect. In this way the coupling of the Gaussian impinging beam and the dc voltage gives rise to director reorientation. Very good agreement is found between the theoretical expectations and the experimental data obtained from SPM experiments.

These results confirm the role of the surface on the supra-nonlinear behavior of the analyzed samples. In particular, the photosensitive dark adsorbed layer of dye molecules acts in the same way as the photoconductive layer of the liquid crystal light valve [23]. Therefore the MR-doped 5CB cell can be a simple alternative to it.

The results reported also demonstrate the possibility of controlling the high optical nonlinearity of our cells in single beam configuration obtaining very high induced birefringence especially in thin samples. The measured nonlinear refractive index in thin samples (10 μ m) is on the order of 0.1 cm²/W and can be varied by more than one order of magnitude by varying the applied voltage of only 1 V. It is our opinion that the results reported can be extremely interesting for the use of liquid crystals in the field of photonic applications.

-
- [1] L. Lucchetti, M. Di Fabrizio, O. Francescangeli, and F. Simoni, *Opt. Commun.* **233**, 417 (2004).
 [2] I. C. Khoo, S. Slussarenko, B. D. Guenther, M. Y. Shih, P. H. Chen, and W. V. Wood, *Opt. Lett.* **23**, 253 (1998).
 [3] B. Y. Zel'dovich, N. F. Pilipetskii, A. V. Sukhov, and N. V. Tabiryan, *JETP Lett.* **31**, 263 (1980).
 [4] F. Simoni, L. Lucchetti, D. E. Lucchetta, and O. Francescangeli, *Opt. Express* **9**, 85 (2001).
 [5] D. Voloshenko, A. Khizhnyak, Yu. Reznikov, and V. Reshetnyak, *Jpn. J. Appl. Phys.* **34**, 566 (1995).
 [6] E. Ouskova, Yu. Reznikov, S. V. Shiyonovskii, L. Su, J. L. West, O. V. Kuksenok, O. Francescangeli, and F. Simoni, *Phys. Rev. E* **64**, 051709 (2001).
 [7] R. Ramos-Garcia, I. Lazo-Martinez, I. Guizar-Iturbide, A. Sanchez-Castillo, M. Boffety, and P. Ruck, *Mol. Cryst. Liq. Cryst.* **454**, 179 (2006).
 [8] L. Lucchetti, M. Di Fabrizio, O. Francescangeli, and F. Simoni, *Opt. Commun.* **233**, 417 (2004).
 [9] L. Lucchetti, M. Di Fabrizio, M. Gentili, and F. Simoni, *Appl. Phys. Lett.* **83**, 5389 (2003).
 [10] L. Lucchetti, M. Gentili, and F. Simoni, *Opt. Express* **14**, 2236 (2006).
 [11] S. D. Durbin, S. M. Arakelian, and Y. R. Shen, *Opt. Lett.* **6**, 411 (1981).
 [12] E. Santamato and Y. R. Shen, *Opt. Lett.* **9**, 564 (1984).
 [13] F. Simoni, *Nonlinear Optical Properties of Liquid Crystals and Polymer Dispersed Liquid Crystals* (World Scientific, Singapore, 1997).
 [14] P. Pagliusi, B. Zappone, G. Cipparrone, and G. Barbero, *J. Appl. Phys.* **96**, 218 (2004).
 [15] L. Lucchetti, M. Di Fabrizio, O. Francescangeli, and F. Simoni, *J. Nonlinear Opt. Phys. Mater.* **11**, 13 (2002).

- [16] E. Ouskova, D. Fedorenko, Yu. Reznikov, S. V. Shiyanovskii, L. Su, J. L. West, O. V. Kuksenok, O. Francescangeli, and F. Simoni, *Phys. Rev. E* **63**, 021701 (2001).
- [17] E. V. Rudenko and A. V. Sukhov, *JETP Lett.* **59**, 142 (1994).
- [18] E. V. Rudenko and A. V. Sukhov, *Mol. Cryst. Liq. Cryst. Sci. Technol., Sect. A* **78**, 875 (1994).
- [19] E. V. Rudenko and A. V. Sukhov, *Mol. Cryst. Liq. Cryst.* **282**, 125 (1996).
- [20] I. C. Khoo, *Mol. Cryst. Liq. Cryst.* **282**, 53 (1996).
- [21] O. Francescangeli, D. E. Lucchetta, S. Slussarenko, Y. Reznikov, and F. Simoni, *Mol. Cryst. Liq. Cryst.* **360**, 193 (2001).
- [22] D. Fedorenko, E. Ouskova, V. Reshetnyak, and Y. Reznikov, *Phys. Rev. E* **73**, 031701 (2006).
- [23] S. A. Akhmanov, M. A. Vorontsov, V. Y. Ivanov, A. V. Larichev, and N. I. Zheleznykh, *J. Opt. Soc. Am. B* **9**, 78 (1992).